

We are IntechOpen, the world's leading publisher of Open Access books Built by scientists, for scientists

6,900

Open access books available

186,000

International authors and editors

200M

Downloads

Our authors are among the

154

Countries delivered to

TOP 1%

most cited scientists

12.2%

Contributors from top 500 universities



WEB OF SCIENCE™

Selection of our books indexed in the Book Citation Index
in Web of Science™ Core Collection (BKCI)

Interested in publishing with us?
Contact book.department@intechopen.com

Numbers displayed above are based on latest data collected.
For more information visit www.intechopen.com



Raman Spectroscopy for Characterization of Hydrotalcite-like Materials Used in Catalytic Reactions

Luciano Honorato Chagas, Sandra Shirley Ximeno Chiaro, Alexandre Amaral Leitão and Renata Diniz

Abstract

This chapter covers a brief review of the definition, structural characteristics and main applications of hydrotalcite, an interesting multifunctional material which finds applicability in different areas. Particularly, some catalytic reactions using hydrotalcite or mixed oxides derived from these materials are addressed (Ethanol Steam Reforming, Photochemical conversions, Hydrodesulfurization). The use of Raman Spectroscopy associated with other techniques, such as powder X-ray diffraction (XRD), Extended X-ray Absorption Fine-Structure (EXAFS), Temperature Programmed Reduction of hydrogen (H₂-TPR), Fourier-Transform Infrared (FTIR) and Density Functional Theory (DFT) simulations, to characterize this type of material is addressed through examples described in the current literature. In this sense, multidisciplinary efforts must be made in order to increase the understanding of the properties of these materials and the catalytic behavior in the most varied reactions.

Keywords: hydrotalcite, heterogeneous catalysis, Raman spectroscopy, nanomaterials, photocatalysis

1. Introduction

Hydrotalcite is a hydroxycarbonate of magnesium and aluminum which occur in nature as a layered double hydroxide (LDH). The LDHs are represented by the general formula $[M^{2+}_{(1-x)}M^{3+}_x(OH)_2]^{x+}(A_{x/n})^{n-} \cdot nH_2O$, where M^{2+} and M^{3+} are divalent and trivalent cations, respectively, and A^{n-} is a charge compensation anion. Their structure consists of brucite-type layers (**Figure 1**), with the substitution of divalent with trivalent cations resulting in a positively charged layer, compensated by interlayer anions [1, 2]. In addition, water molecules are present in interlayer spaces collaborating for the stabilization of the crystalline arrangement through varying hydrogen bonds.

The mineral hydrotalcite has the molecular formula $Mg_6Al_2(OH)_{16}CO_3 \cdot 4H_2O$, however, the synthetic hydrotalcite-like materials can have a wide compositional cation variability, different cationic ratios and varying anions in the interlayer region.

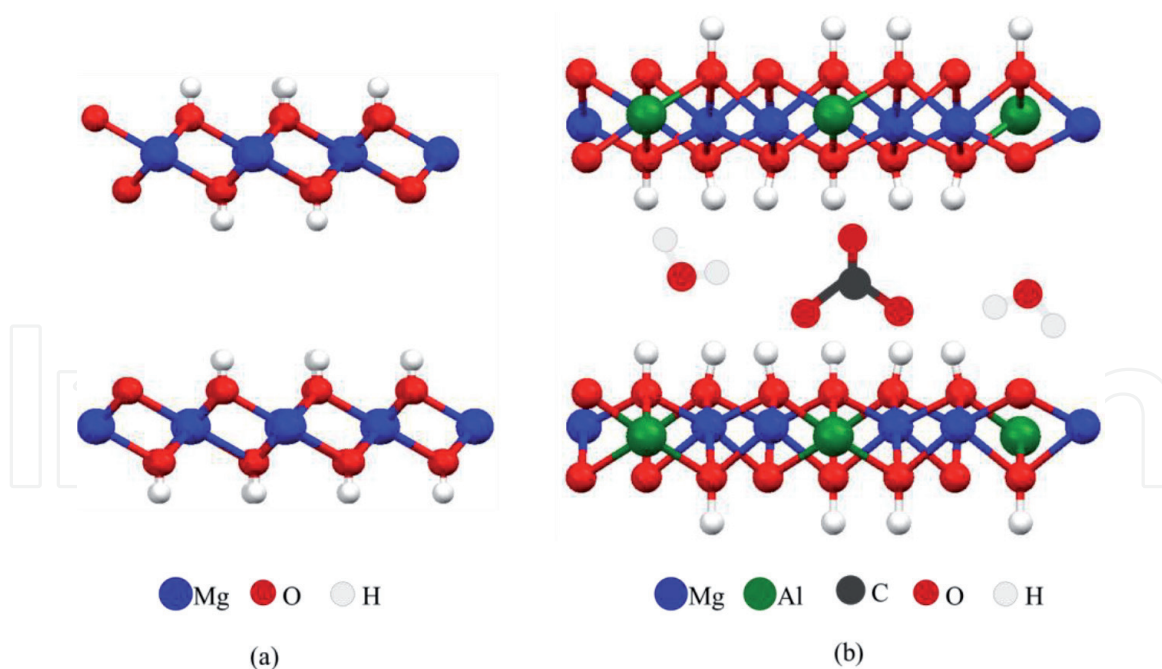


Figure 1.
Schematic representations of (a) Brucite and (b) Hydrotalcite.

Undoubtedly the LDH most used in several applications is the MgAl-LDH system containing carbonate as interlayer ions. However, several other cations and anions are part of countless possible compositions. Co-precipitation is the main preparation method of LDHs, which consists of slowly adding an aqueous solution containing the metal ions in a proper ratio over an aqueous solution containing the hydroxyl ions (usually NaOH) and the anion to be intercalated under vigorous stirring during a certain time. The obtained precipitate is filtered, washed with deionized water, and dried. This is the least cost method for producing LDH. Mostly the production requires strict control of temperature, stirring, and pH to avoid the formation of impurities such as simple hydroxides. In the industrial case, the separation of impurities can raise the price of the final product.

These materials can be prepared by several methodologies other than co-precipitation. An alternative is the hydrothermal method, which permits obtaining high particle size and high product purity [3, 4]. This method is similar to the co-precipitation, meantime, after stirring the suspension is transferred to a Teflon autoclave for hydrothermal treatment. The temperature and aging time influences directly in the crystallinity and morphology uniformity of the material [3–8]. Urea hydrolysis is a satisfactory example of hydrothermal synthesis in which urea is used as a source of carbonates and hydroxyls anions, providing better crystallinity due to very slow precipitation [9–11].

The ion exchange method is widely used; mainly for the intercalation of drugs [12, 13]. This method consists of inserting the precursor LDH in an aqueous solution containing the anion to be intercalated. The exchange of anions in the interlamellar space occurs after pH adjustment and constant stirring, generating a new LDH after the experimental procedures. The solid precipitate is then filtered, washed with deionized water, and dried in an oven. Increased interlayer distance may occur depending on the size of the intercalated ion, as exemplified in **Figure 2**.

The LDHs reconstruction method is known as the memory effect, an intrinsic property of this type of material, which is characterized by the regeneration of the lamellar structure after thermal decomposition (**Figure 3**).

The thermal decomposition of this type of material is a complex sequence of steps that involve dehydration, dehydroxylation (loss of hydroxyls), and loss of

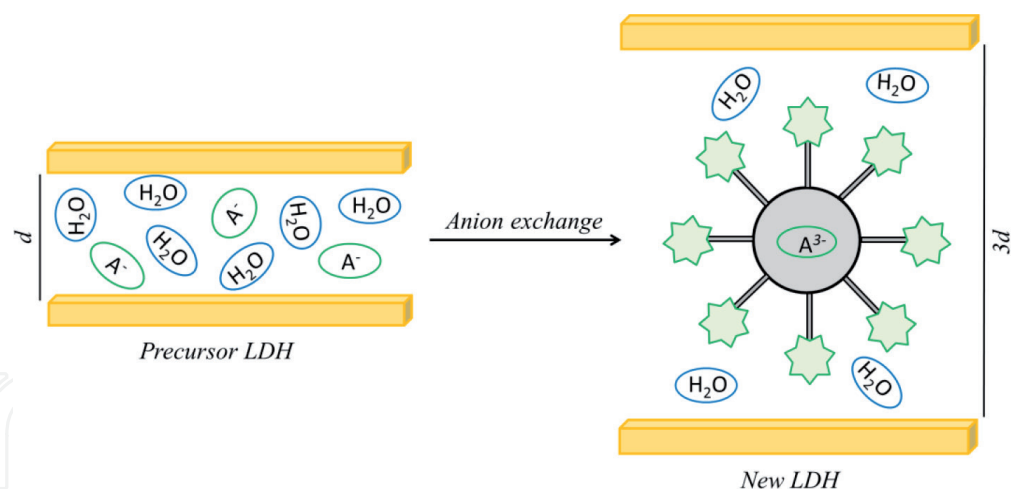


Figure 2.
Schematic representation of ion exchange method.

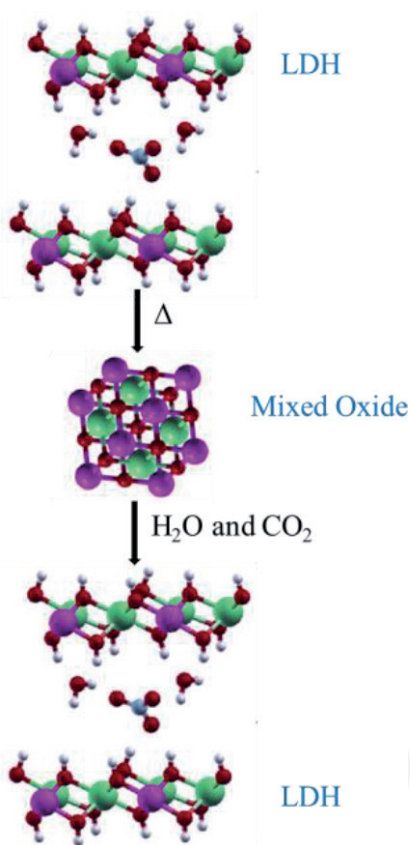


Figure 3.
Schematic representation of memory effect.

carbonate in the starting material [14]. The initial lamellar structure forms mixed metal oxides as the final products of thermal decomposition. When subjected to hydration, these oxides are capable of regenerating the initial lamellar structure. This method can also be used for ion exchange, since the solution used for rehydration may contain anions different from those contained in the initial LDH.

In addition to the aforementioned methodologies, the following deserve mention: sol-gel synthesis [15, 16], salt oxide method [17, 18], sonochemical assisted synthesis [19–21], and manual grinding method [22, 23]. The methodologies mentioned here do not exhaust the possibilities of synthesis of LDH. It should be noted that each method has its advantages and disadvantages and can be improved and applied according to the specifics of the desired product.

2. Applications of hydrotalcite-like materials

The great current interest in LDHs is due to the wide range of possible applications in different areas. This is reflected in a large number of recent reviews and papers published in high-impact journals from a variety of research fields. In the biomedical area, for example, Shirin *et al.* [24] described recent advances in the structure, properties, synthesis, functionalization, and drug delivery applications of LDHs. It was emphasized that compared to other nanomaterials, LDHs are better candidates for release a drug/gene in a controlled manner and deliver them efficiently in the target sites. This is due to its structure and high surface volume ratio. Moreover, the stability in a definite pH range, biocompatibility, high loading, and high anion exchange capacities improve the bioavailability and allow slow release of intercalated drug decreasing the frequency of drug administration.

Jin *et al.* [25] reported that the physicochemical properties of the LDH nanoparticles favor the high biocompatibility and low toxicity for use in the human biological system. The synthetic MgAl-LDH Talcid®, from Bayer, is a traditional example of this field. This worldwide commercialized stomach antacid and anti-pepsin has a structure analogous to that of the hydrotalcite mineral, being able to keep the stomach pH stable between 3 and 5. The intercalation of LDHs with anionic biomolecules, forming the so-called hydrotalcite nanohybrids, is also addressed in the work of Jin *et al.* [25]. DNA, small interfering ribonucleic acid (siRNA), anti-cancer drugs, and contrast agents are among the anionic bioactive molecules that can be intercalated in the hydrotalcite structure. Because it is naturally sensitive to the biological acid medium, LDH allows for controlled drug/gene delivery. In addition, its physicochemical properties such as particle size and morphology can be controlled by varying the synthesis conditions, enabling the minimization of toxicity.

Still, in relation to the use of LDHs in the biomedical area, Meirelles and Raffin [26] published a technological and scientific prospection related to patents and articles involving composites employed in therapeutic devices. Despite the growing interest in the area, the authors considered the number of patents low (on average less than 10 documents per year in the last decade), and attributed this to the lack of regulation on nanomaterials used in the development of medications. Additionally, for further advances in nanomedicine applications are necessary: to improve the synthesis methodologies to enable uniform particle size distribution; understand how the number/density of surface modifiers affects biological performance; increase the molecular selectivity; study long-term side effects; to develop diverse imaging modalities for studies at molecular level providing comprehensive biological information; and to develop functional LDHs loading multiple antigens and biological adjuvants [27].

Another extremely relevant sector where LDHs are widely used is the removal of contaminants from water. Access to clean water and an efficient basic sanitation system are essential factors for socioeconomic development and the reduction of millions of deaths annually worldwide. Certainly, this situation is further aggravated by the pandemic caused by the new corona virus. Moreover, the need for decontamination of rivers and fountains is increasing, due to pollution caused by industrial and human waste. In this sense, LDHs have been extensively researched for use in water purification [28–30]. Its anion exchange property associated with high surface area, compositional versatility, and higher adsorption capacity are characteristics that differentiate them from other mineral adsorbents such as aluminum or iron oxy-hydroxides [28]. Nevertheless, scientists in this field agree that more knowledge is needed to be able to apply these materials on a large scale [28–31]. Techniques of preparation, functionalization and thermal activation must

be improved aiming to increase the understanding of their behavior on an atomic scale. In this way, it will be possible to correlate structure, chemical composition, morphology, and surface properties to maximize the adsorption capacity and, consequently, achieve better performances in removing pollutants from water.

Polymer nanocomposites (PNCs) containing LDHs are also considered as an important alternative for water purification systems. These materials have the interesting ability to combine the characteristics of the polymeric matrix and the LDH, forming nanocomposites with multifunctional properties. Pandey *et al.* summarized eight methods used to water decontamination: adsorption, coagulation and flocculation, membrane separations, ion exchange, oxidation, advanced oxidation process, biodegradation, and microbial treatment [32]. The authors stated that is required a combination of processes to insure adequate quality of water, and PNCs can be used in all these processes, permitting efficient decontamination of metal ions, dyes, and microbes. Excellent arsenic absorption and regeneration ability were reported for PNCs, and factors like synthesis, calcination and LDH composition were pointed as crucial for achieve a better performance [33]. Wang *et al.* synthesized a functionalized hydrotalcite/graphene oxide hybrid nanosheets and used as nanofiltration membrane for water desalination. The exfoliated hydrotalcite and graphene oxide were incorporated into polyamide membrane, generating a material with singular characteristics, achieving enhanced water flux and superior water softening performance [34]. However, according to Mohapi *et al.* [31], there are challenging conditions for these materials to be manufactured and used efficiently, such as: the selection of appropriate nanomaterials that possess specific interfacial interaction, the compatibility of nanomaterials with polymer matrix, and the homogeneous dispersion of LDH particles in the polymeric matrix. Given the above, the use of LDHs or PNCs for water contaminants elimination requires a multidisciplinary knowledge of characterization techniques, whether they are X-ray diffraction, microscopic or spectroscopic.

The great interest in the application of LDHs and their composites with various substances is not limited only to the mentioned areas. A series of possible preparations, characterizations, and industrial applications were exemplified in some interesting reviews [35, 36]. The review of Yan *et al.* report the use of these materials in the selective catalytic reduction of NO_x with NH_3 , which is one important task for non-power industry (steel, cement, waste incineration, etc.), capable of enabling energy conservation and emission reduction [37]. The uniform interlayer galleries of the LDHs allow its application as membranes for gas/liquid separations [38]. Their excellent anion exchange capacity stimulates the use as host-guest materials applied in the pesticide-related field [39]. The improved thermal, mechanical and rheological properties of PNCs containing LDHs significantly enhance the performance on flame retardancy and physical properties of the paper and epoxy resin [40, 41]. Low cost plastic films can be produced and used in agricultural area. The work of Xie *et al.* showed that PNCs composed by low density polyethylene and intercalated LDH with lauryl phosphoric acid ester potassium can be applied for this purpose [42]. Charttejee *et al.* reported the synergistic effect present in bionanocomposites made from LDH and different biopolymers [43]. The importance of this theme is related to environmental protection, since biopolymers are environment friendly, fully degradable and sustainable materials. In the area of fertilizers, for example, Borges *et al.* [44] stressed the importance of new methods or products to achieve improvements in the management of nutrients and to reduce environmental impacts. The use of LDHs for corrosion protection of aluminum alloys has also been identified as a new alternative to replace chromate-based coatings due to the harmful action of chromium species on human health and the environment [45]. Electrochemical

capacitors, or supercapacitors, based on LDHs also have been studied as novel and sustainable energy storage technology [46]. Furthermore, the structural characteristics of hydrotalcite-like materials are identified as suitable for use as building materials in the construction industry in addition to factors such as low cost and high availability in mineral reserves [47]. Thus, LDHs find applications in these and in several other fields of research. In the next section, emphasis will be placed on its use in catalytic reactions.

3. Some catalytic reactions using hydrotalcite or mixed oxides derived from these materials

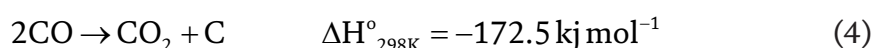
One of the areas in which LDHs find wide application is in catalysis. Particularly, in heterogeneous catalysis and photocatalysis, the LDHs are very used as a catalyst or, mainly, as a precursor of mixed oxides, which, in turn, can be used in various industrial catalytic processes [48–54]. Below will be highlighted some interesting catalytic reactions using hydrotalcite-like materials as catalyst or catalyst precursor. Examples of how Raman spectroscopy can be used to characterize these materials will also be discussed.

3.1 Ethanol steam reforming

The use of hydrogen as an alternative to fossil fuels is an area of great interest to industries, governments, and researchers worldwide. In addition to its pollution-free characteristic, the high energy value and rich resources further enhance research on this subject. The catalytic steam reforming is the technology applied industrially for the hydrogen production. Light hydrocarbons are used in this process, especially methane. In this case, the reaction occurs in two steps: firstly, methane reacts with water vapor generating CO and H₂; after, CO undergoes water gas shift (WGS) reaction generating CO₂ and more H₂ Eqs. (1) and (2).



An alternative for the hydrogen production is the use of alcohols as source. Particularly, in relation to other alcohols, ethanol has some advantages from a socio-environmental point of view, such as ease of obtaining from renewable sources, large volume of production due to existing industrial facilities, ease of handling, and being non-toxic. The Eq. (3) summarizes the global ethanol steam reforming (ESR) reaction, but several other reactions such as WGS Eq. (2) and Boudouard reaction Eq. (4) occur concurrently [55].



Several systems are tested in the ESR reaction and the most relevant results are obtained for catalysts containing noble metals such as Pt, Pd, Ru or Rh [56, 57]. On

the other hand, Ni, Co or Cu based catalysts can provide a better cost–benefit ratio. However, the greatest impediment to the industrial use of this process is to control the secondary reactions that occur and lead to the deactivation of the catalyst. The resolution for this involves the development of active, selective, and stable catalysts. Thus, mixed oxides formed from LDHs have been used for this purpose.

Passos *et al.* [58] combined Quick-EXAFS and Raman spectroscopies in *operando* conditions to monitoring activation, reaction, and deactivation of NiCu catalysts obtained from hydrotalcite-like precursors. The catalyst activation was performed by heating the LDH precursor under two steps. Firstly, the LDH precursor was calcined under air atmosphere until 210°C. After purge with He, the material was further heated up to 500°C under 5% of H₂/He in order to form the metallic nanoparticles. The EXAFS and XANES analyzes showed that the activation method used is more efficient than the conventional one, as it completely reduces the copper and nickel particles producing metallic particles at lower temperatures.

Raman and mass spectroscopies were used to monitoring the evolution of ethanol conversion and products obtained during the ESR reaction. Full conversion was achieved during the initial 30 min, however several byproducts were observed revealing the occurrence of parallel reactions. After 50 min a decrease in ethanol conversion is accompanied by a decrease in selectivities to CO₂ and H₂. The catalyst deactivation was monitored by increase of D and G bands observed respectively at 1336 and 1586 cm⁻¹ in Raman spectra. These bands are respectively characteristics of large aromatic ring systems and ordered graphitic carbon species. Concomitantly, mass spectroscopy showed that these coke deposits originate from decomposition reactions of ethylene, acetaldehyde, and methane, in addition to the polymerization of ethylene and the Boudouard reaction. Besides filamentous and graphitic, amorphous coke species also were detected by Raman analysis, reaching 30% of coke deposits after 180 min on stream. The amorphous coke species were identified through vibrations at 1278 and 1500 cm⁻¹, by deconvolution of Raman signals. These species come from acetaldehyde and ethylene reactions, and encapsulate the metallic sites accelerating the deactivation process. Oxidative regeneration was performed and ESR reaction was restarted. Then, metallic particles were recovered (100% of Cu⁰ and 85% of Ni⁰) due to the H₂ formed in the ESR reaction, leading to a second reaction cycle with performance equivalent to the first one.

Sikander *et al.* published a detailed review addressing the hydrogen production using hydrotalcite based catalysts [59]. Besides ESR reaction, emphasis was given to reactions such as: methane steam reforming, methanol steam reforming, dry reforming of hydrocarbons, methane partial oxidation, and sorption enhanced reaction process. The authors highlighted that the main drawback in conventional hydrogen production systems is the high carbon deposition on catalytic surface. In this sense, it is necessary to produce in situ catalytic regeneration conditions. Undoubtedly, the work of Passos *et al.* [58] represents a contribution in this regard. Indeed, the structure and high surface area of the LDH based catalysts are physicochemical characteristics that make these materials able to overcome these challenges. New compositions and the association of LDHs with other materials, forming nanocomposites, are pointed out as the future of catalysts for hydrogen generation.

3.2 Photochemical conversions

During a photocatalytic process, a semiconductor surface is excited by ultraviolet–visible radiation. After absorbing energy equivalent to or greater than its band gap, an electron (e^-) is promoted from the valence band (VB) to the conduction band (CB), where holes (h^+) are produced. Then, photocatalytic reactions occur

through charge conductors, derived from this electronic promotion between bands, leading to the reduction of molecules adsorbed by the excited electrons present in the CB or to the oxidation of molecules by the positively charged holes in the VB (**Figure 4**). Thus, the generation of photoactivated electron–hole pairs allows conducting a widespread range of important chemical reactions [60–64] in an economical and environmentally sustainable manner as alternative to substitute the traditional processes. Because of low costs, recyclability capacity, wide light absorption range, and adjustable band gap, the hydrotalcite-like materials are intensively studied as photocatalysts.

As mentioned in Section 2, LDHs can be used for water purification. Major sources of environmental contamination are found in industrial waste, mainly from the dyeing industries, leading to problems such as low biodegradability, changes in color, smell and pH, in addition to low oxygen availability. The biological treatment is the most used for decontamination of water containing dyes, however it is considered slow and several poisonous molecules cannot be biologically treated. Other techniques are considered expensive and not all the usual techniques are capable of efficiently eliminating all toxic elements. In this regard, photocatalysis emerges as an alternative, enabling the development of more efficient and less environment harmful systems.

De Carvalho *et al.* [65] carried out the application of a niobium oxide catalyst supported on mixed oxide derived from LDH in the photodegradation of the methylene blue dye. The synthesis of ZnAl-LDH was performed by co-precipitation. After thermal decomposition, the precursor generated a mixed oxide, which was submitted to wetness impregnation for incorporation of niobium oxide. In the tests, after only three hours of sun exposure, the applied catalyst led to almost 100% degradation of the dye without the need for any additives. After degradation, the catalyst was recovered and reapplied in another three reaction cycles without significant loss of catalytic activity. This study showed the importance of using photocatalysis in advanced oxidation processes as a method for destroying water polluting molecules.

In another work, De Carvalho *et al.* [66] tested this system in oxidative and photochemical conversion of anilines to azoxybenzenes. Beyond ZnAl, MgAl and MgZnAl-LDH were also synthesized and tested as supports for niobium oxide, yet MgZnAl catalyst was more successful, leading to azoxybenzenes yields up to 92%. The XRD patterns showed wide profiles associated to mixed oxides with low crystallinity. In this case, the presence of niobium species on the support surface was verified through Raman spectroscopy coupled to an optical microscope with a CCD detector. The Raman mapping was measured in the region characteristic of

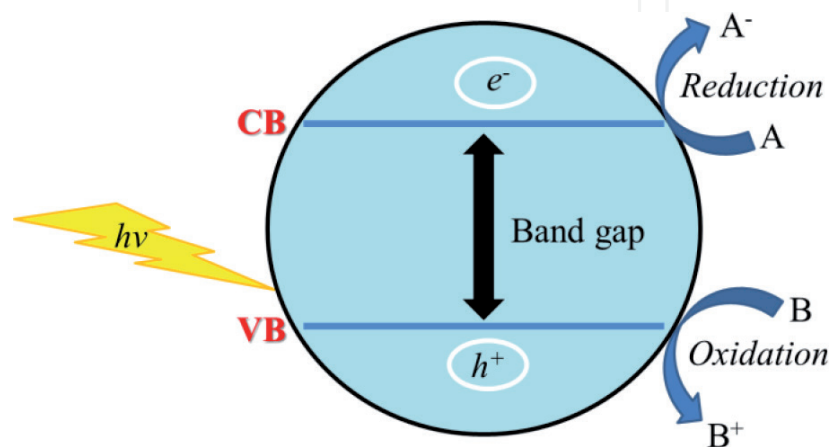


Figure 4.
Schematic representation of a reaction catalyzed by a semiconductor.

niobium oxides (between 960 and 750 cm^{-1}). Integration of this area revealed that the relationship between zinc content and surface area is inversely proportional. This directly affects the dispersion of niobium oxide on the support surface, because the greater the amount of zinc in the support, the greater the number of NbO_x clusters, that is, the lesser the dispersion. However, even with heterogeneity in the active phase distribution, the most effective catalyst was the one impregnated on the mixed oxide derived from MgZnAl-LDH. DFT calculations and acid-basic characterization tests showed that the balance between acidic and basic sites is responsible for the greater activity of this catalyst. Moreover, DFT calculations revealed that the charge transfer between nitrogen of aniline and niobium is the first step of the mechanism of photocatalytic synthesis of azoxybenzenes, suggesting chemisorption between the reactant and the catalyst surface. Anyway, this work is an example of how multidisciplinary efforts should be used to characterize materials and understand reaction mechanisms.

3.3 Hydrodesulfurization

In order to improve the air quality, governments in various countries have announced new regulations to reduce the level of sulfur, nitrogen, and other contaminants which are present in transportation fuels [67]. Therefore, refiners need to decrease the concentration of contaminants, particularly in gasoline and middle distillates [68]. Gasoline from fluid catalytic cracking (FCC gasoline), which represents 30–50% of the total gasoline pool, is by far the most important sulfur contributor in gasoline, up to 90% [69]. Although, the olefins, which are important contributors to the octane rating in commercial petrol, are also present in FCC fraction. As a result, FCC gasoline is the focus for sulfur reduction.

The conditions used in the catalytic hydrodesulfurization (HDS) process such as high pressure, high temperature, and high hydrogen consumption make the process expensive. Several alternative methods, such as adsorption or alkylation have been developed in recent years. However, the key technical problem for the HDS of FCC gasoline is to perform a deep sulfur removal and, at the same time, to reduce the loss of the olefins occurring in the HDS process, by minimizing the hydrogenation (HYD) [70].

To preserve the olefins responsible for the octane number, it is necessary to improve the selectivity of the conventional catalysts (sulfide CoMo/ γ -Al₂O₃) without loss of octane number. In this connection, one of the key parameters which determine the activity of the CoMo HDS catalysts is the type of support. Aiming to reduce the loss of octane number, Zhao *et al.* [70] used sulfide CoMo catalysts supported on the MgAl, CuAl and ZnAl mixed oxides obtained from hydrotalcite compounds. The authors observed that the catalysts give lower levels of olefin hydrogenation than the traditional γ -Al₂O₃ supported catalyst. In this sense, Coelho *et al.* reported a series of papers devoted to the preparation, characterization and catalytic evaluation of CoMgMoAl catalysts derived from LDHs [71–73]. Initially, the co-precipitation method was used to prepare terephthalate-intercalated CoMgAl-LDH. Next, the anion exchange process was used to substitution of terephthalate by polyoxometalate and preservation of the LDH structure. Then, the calcination of this LDH generates CoMgMoAl mixed oxide, which is precursor of the sulfide active phase. The sulfide characterizations and catalytic tests showed that olefin hydrogenation is associated with un-promoted Mo sites while the improvement in activity and selectivity for HDS is due to the increase in the number of Mo sites promoted by Co.

Presently, we characterize an MgAl-LDH and evaluate the use of their derived mixed oxide as support for HDS catalyst in comparison with γ -Al₂O₃. The powder

X-ray diffraction (XRD), BET, Temperature Programmed Reduction of hydrogen (H_2 -TPR), and Fourier Transform Spectroscopies (FTIR and FT-Raman) were used to characterize the materials. FTIR spectra were recorded on a BOMEN MB-102 spectrometer using pressed KBr pellets and 4 cm^{-1} of spectral resolution to verify the vibrational modes present in the samples. Good signal-to-noise ratio was obtained from the accumulation of 128 scans. Raman spectra were acquired on a LabRAM HR-UV 800/Jobin-Yvon equipment, with He-Ne (633 nm) laser and CCD detector. The resolution was 2 cm^{-1} in the range between 1200 and 100 cm^{-1} . Moreover, the hydrodesulfurization of thiophene and hydrogenation of cyclohexene were the reactions chosen to evaluate the activity and selectivity of CoMo sulfide catalysts.

The MgAl-LDH and Boehmite are commercial samples provided by Petrobras-Cenpes. These samples were calcined at 500°C for 3 h under air, to obtain the oxide supports (named as MgAl and $\gamma\text{-Al}_2\text{O}_3$, respectively). The supports were submitted to incipient wetness impregnation of solutions containing the Mo and Co salts using the appropriate amount of ammonium heptamolybdate and cobalt nitrate, to obtain catalysts with 10% of MoO_3 and 3% of CoO on the surface. After calcination at 450°C for 1 h, the oxide catalysts were denominated CoMo/MgAl and CoMo/ $\gamma\text{-Al}_2\text{O}_3$.

The spectroscopic data obtained for the MgAl-LDH are shown in **Figure 5**. In the FTIR spectrum, the strong and wide absorption band centered at 3464 cm^{-1} is due to the contribution of the asymmetric stretching modes of the lamellar hydroxyl groups (ν_{OH}) and of the interlamellar water molecules [74]. The shoulder at 3085 cm^{-1} is characteristic of the ν_{OH} symmetrical stretching of water molecules interacting by hydrogen bonding with interlamellar carbonate ions. The poor absorption at 1633 cm^{-1} is attributed to the deformation mode of water molecules (δ_{OH}). The band at 1354 cm^{-1} is assigned to the asymmetric stretch mode, ν_3 , of carbonate, and the small band at 1074 cm^{-1} is assigned to the symmetrical mode, ν_1 , of carbonates connected to OH groups, as suggested by absorption around 3000 cm^{-1} . This absorption is expected due to the decrease in the symmetry of the carbonate groups (from D_{3h} to C_{2v}), caused by different types of interaction of these anions with interlamellar water molecules and hydroxyl groups present in brucite-like layers [75, 76]. The band at 775 cm^{-1} corresponds to the mode of deformation outside the plane of carbonate ions, and the mode of deformation in the plane is

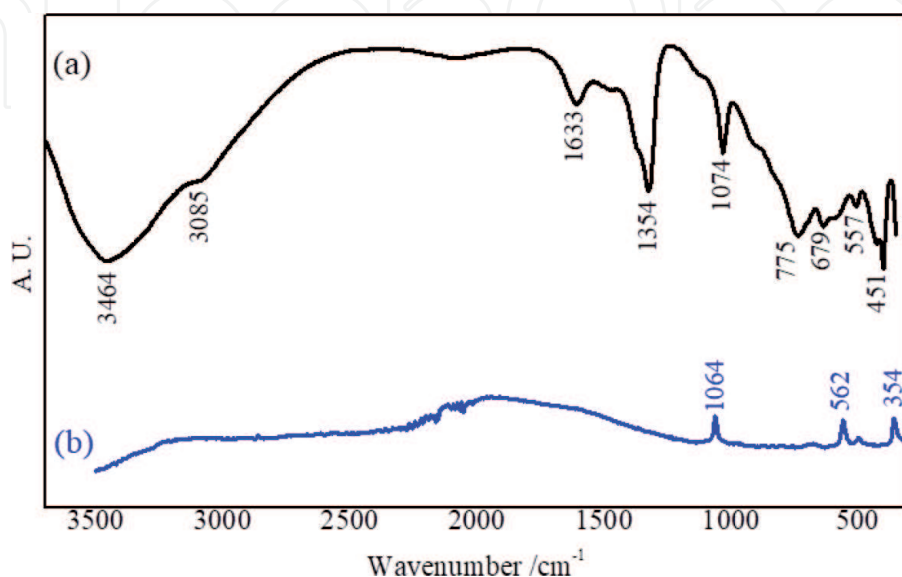


Figure 5.
FTIR (a), and FT-Raman (b) spectra of MgAl-LDH.

observed at 679 cm^{-1} . Still in the region of low wavenumber, the absorption around 557 cm^{-1} is attributed to the vibration of the carbonate-water units [76], however this absorption can also be attributed to the M-O-M, O-M-O, and M-OH lattice vibration modes (where M is Mg or Al) [77]. Finally, the 451 cm^{-1} band is attributed to the contribution of the Mg-O and Al-O stretching modes.

All data obtained through infrared analysis are in agreement with that observed in the FT-Raman spectrum. This spectrum features three typical LDH bands [76, 78]. The three weak absorptions at 1064 cm^{-1} , 562 cm^{-1} , and 354 cm^{-1} are attributed as symmetrical stretching of the carbonate ion, CO_3^{2-} units linked by hydrogen interaction to interlamellar water molecules, and Mg-O stretching, respectively. Therefore, the vibrational study carried out using infrared and Raman spectroscopies suggests that carbonate ions are present in the crystalline network of the sample and are involved in hydrogen bonds.

In the infrared spectrum of the Boehmite sample, it is verified the presence of a band at 3315 cm^{-1} commonly attributed to the asymmetric stretching modes ν_{OH} from water molecules and hydroxides (Figure 6a). In addition, a band at 3094 cm^{-1} is observed due to the symmetric stretching ν_{OH} of hydroxyl groups interacting through hydrogen bonds. Around 1639 cm^{-1} , absorption attributed to the δ_{OH} mode is noted. The $\delta_{\text{Al-OH}}$ mode is observed at 1074 cm^{-1} . The $\nu_{\text{Al-O}}$ vibrational modes, with maximum absorption at 625 cm^{-1} , appear as part of a wide and intense band in the region between 900 and 600 cm^{-1} , which in turn still contains the contribution of lattice vibrational modes [79].

In the Raman spectrum (Figure 6b), the 680 and 500 cm^{-1} bands are assigned to the asymmetric and symmetric stretch modes $\nu_{\text{Al-OH}}$, respectively. In addition, the intense band at 364 cm^{-1} stands out, due to the $\nu_{\text{Al-O}}$ stretching mode. Thus, these results corroborate with the infrared analysis, suggesting that the sample has a typical Boehmite spectrum.

All the peaks in the XRD patterns were indexed (Figure 7) [9, 80–84]. The cell parameters for the MgAl-LDH were refined using the Checkcell software [68] (Table 1). The input values were $a = 3.0424$ and $c = 22.6641\text{ \AA}$ of a rhombohedral $R\text{-}3m$ space group. The interlayer distance value calculated from the more intense reflection (d_{003}) is consistent with the values found in the literature [9, 81].

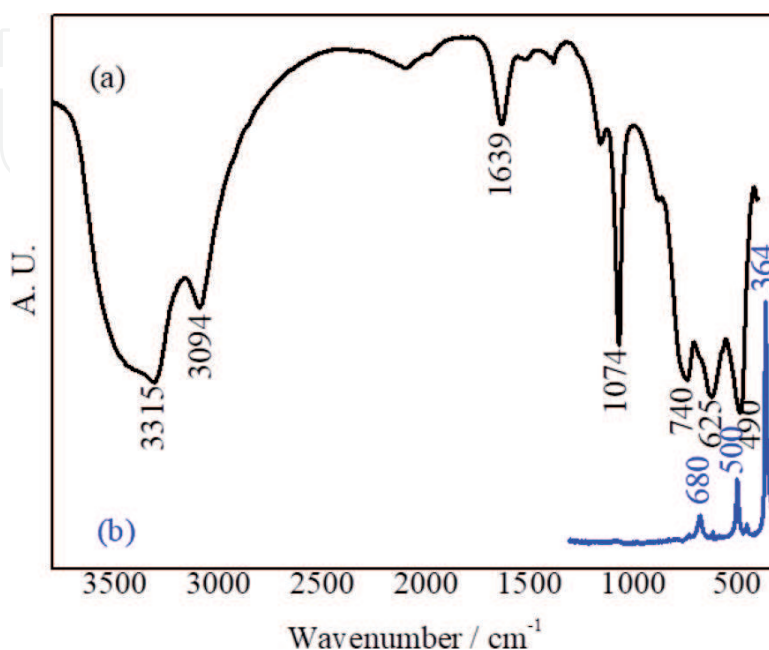


Figure 6.
FTIR (a), and FT-Raman (b) spectra of Boehmite.

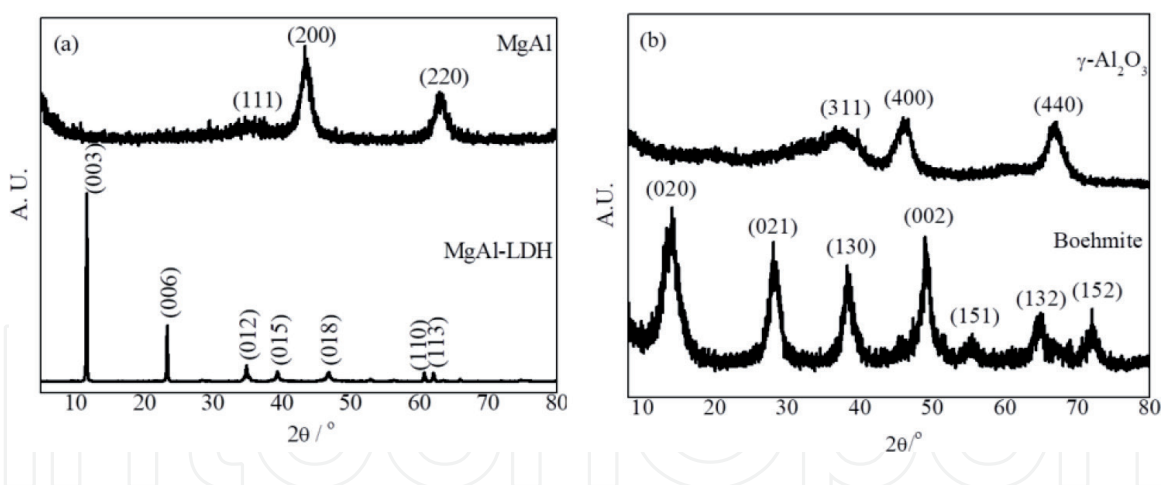


Figure 7. X-ray diffraction patterns of (a) MgAl-LDH and MgAl, and (b) Boehmite and γ -Al₂O₃.

CS (nm)	<i>a</i> (Å)	<i>c</i> (Å)	<i>d</i> ₀₀₃ (Å)	Support	CS (nm)	<i>a</i> (Å)
56.8	3.026 (7)	22.607 (5)	7.49		11.4	4.149 (4)

Table 1. Crystallite size (CS) and lattice parameters for MgAl-LDH and its derived mixed oxide.

Subtraction from this value of the brucite layer width (4.80 Å) provides an interlayer spacing around 2.70 Å, which is of the same order of magnitude of the size of carbonate anions in vertical orientation. This result agrees with Raman and FTIR data and suggests that these anions have reduced mobility in the crystal lattice as they are involved in strong electrostatic interactions with lamellar hydroxyls and water molecules located in the interlayer spaces [82, 83]. The other precursor exhibits a typical Boehmite profile; consisting of an orthorhombic unit cell with space group *Cmcm* [84–86].

The diffraction patterns obtained for the supports are also show in **Figure 7**. The XRD profile of MgAl mixed oxide is typical of rock-salt phase [87–89]. The cell parameter *a* (**Table 1**), lower than the pure MgO (4.211 Å), suggests an isomorphous Mg²⁺/Al³⁺ substitution, giving rise to an oxide solid solution containing Mg and Al [87–89]. In turn, the calcination of Boehmite led to the formation of γ -Al₂O₃, with spinel-type structure (*Fd-3m* space group).

The XRD patterns obtained for both CoMo catalysts show no major differences relative to the respective supports, despite the decrease of the peak intensities, indicating a decrease in crystallinity after impregnation (**Figure 8**). This aspect indicates good dispersion of the impregnated phases in accordance with surface areas, which decreased slightly in relation to the supports (from 191 to 175 m²g⁻¹ for CoMo/MgAl, and from 240 to 201 m²g⁻¹ for alumina based catalyst). However, in this case, the XRD technique does not allow the identification of the crystalline phases present on the supports. For this, Raman spectroscopy is extremely useful.

Typical Raman spectrum of the supported CoMo oxide catalysts is shown in **Figure 9**. The main bands around 995, 818, 665, 378, 337 and 291 cm⁻¹ are characteristics of MoO₃ [90, 91]. The most intense bands at 995 cm⁻¹ and 818 cm⁻¹ correspond to symmetric ($\nu_{\text{Mo-O}}$) and asymmetric stretching ($\nu_{\text{Mo-O-Mo}}$) vibrational modes, respectively [92]. Additionally, a low intense band assigned to CoMoO₄ phase is observed at 950 cm⁻¹ [93]. The CoMoO₄ oxide is known as a good precursor for HDS catalysts, because it could lead to the formation of the active CoMoS Type II phases [94]. Thus, the Raman spectrum suggests that CoMoO₄ and MoO₃ species coexist on the surface of the supported CoMo oxide catalysts.

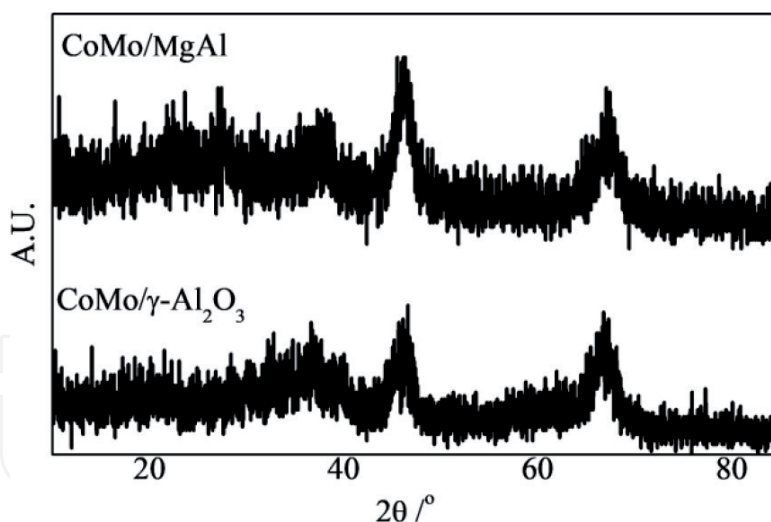


Figure 8.
X-ray diffraction patterns of the CoMo catalysts.

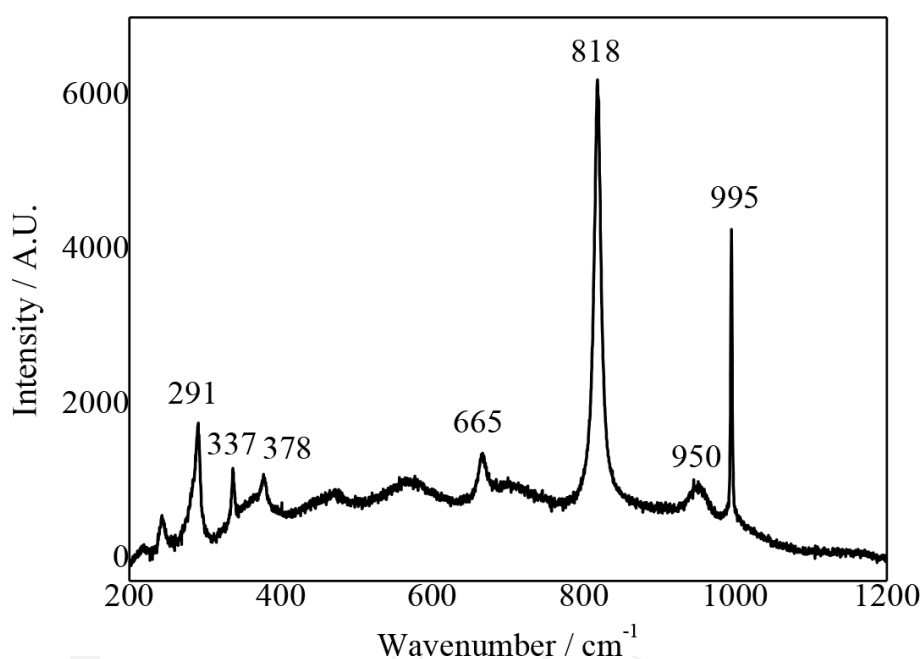


Figure 9.
Raman spectrum of CoMo/ γ -Al₂O₃ catalyst.

H₂-TPR technique was used to verify the reduction behavior of impregnated species on the supports. **Figure 10** shows the H₂-TPR profiles of supported oxide catalysts. The CoMo/MgAl catalyst exhibit two peaks (375 and 556°C), while the CoMo/ γ -Al₂O₃ catalyst display a peak at 460°C. In the literature, was reported that for catalysts containing only cobalt oxide dispersed on alumina (Co/ γ -Al₂O₃) there is a peak around 340°C, assigned to the reduction of Co₃O₄, and peaks between 600 and 700°C, attributed to the reduction of Co²⁺ ions in different chemical environments [95]. When there is only molybdenum oxide on alumina (Mo/ γ -Al₂O₃), the Mo⁶⁺ → Mo⁴⁺ reduction generally occurs at 500°C. This indicates that Mo⁶⁺ cations are easily reduced. Moreover, commonly above 800°C, are observed peaks related to different reduction steps (MoO₃ → MoO₂ → Mo⁰) [96, 97].

H₂-TPR profiles obtained in the present work suggest an interaction between cobalt and molybdenum species, considering that the first peak is observed between 375 and 460°C (temperature higher than Co/ γ -Al₂O₃ and lower than Mo/ γ -Al₂O₃ reductions). Furthermore, for both samples the second reduction occurs above

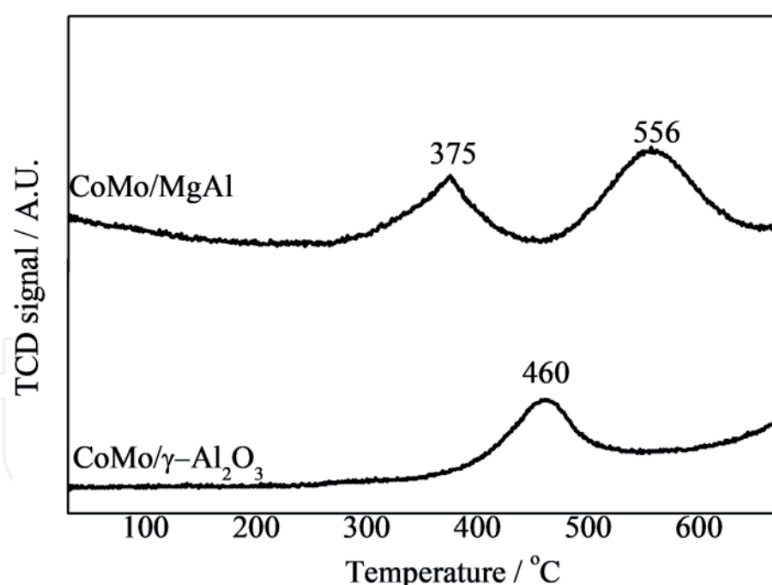


Figure 10.
H₂-TPR profiles of CoMo catalysts.

800°C. The species reducing at slightly higher temperatures may have a somewhat stronger interaction with support surface. Thus, they cannot be reduced and they are therefore probably lead to inactive phases in the HDS reaction. Similar profile is observed in the work of Liu *et al.* [95], suggesting the formation of CoMoO₄ in addition to MoO₃ on both supports, corroborating the Raman results showed earlier. It is also observed that the reduction occurs primarily for the sample supported on mixed oxide derived from LDH. This suggests that the interactions of impregnated species with this support are weaker than with γ -Al₂O₃. Additionally, the hydrogen consumption in H₂-TPR analyses is 1.8 and 2.2 mmol g⁻¹ for CoMo/MgAl and CoMo/ γ -Al₂O₃ respectively. This consumption is directly related to the amount of CoMo reducible species on the surface, which can be related to HDS activity.

For catalytic tests, the reactor was loaded with 300 mg of supported oxide catalyst and 900 mg of SiC (both 80–100 Tyler mesh) between quartz-wool plugs. The pre-sulfiding of the supported oxide catalysts was carried out according to the following procedure: initially, the materials were dried at 150°C for 30 min under a 450 mL min⁻¹ nitrogen flow. Then, the supported oxide catalysts were presulfided using a mixture of 1.66% CS₂ in n-heptane (v/v). The liquid was fed to the reactor at 20 mL h⁻¹ under hydrogen flow (450 mL min⁻¹) and at atmospheric pressure. The sulfidation temperature was maintained at 280°C for 1 h, at 350°C for 30 min and, finally, at 400°C for 30 min. After sulfidation, the catalysts were tested at 280°C and 20 bar. The liquid feed consisting of 0.8% of thiophene and 17% of cyclohexene in n-heptane (v/v) was pumped to the reactor at 16.8 mL h⁻¹ with a 450 mL min⁻¹ hydrogen flow. The conversions were kept low in order to operate in differential regime.

The results show that the tested catalysts are active for both, HDS and HYD reactions, for which the main products were butenes and cyclohexane, respectively. Previous studies described calculations methods for the conversions of thiophene HDS and cyclohexene HYD, which were performed from the carbon balance for each of the reactants and the respective reaction products [73]. The results of catalytic performances are displayed in **Figure 11**. It is important to mention that the activity for HDS is practically the same for both catalysts, since thiophene conversions are around 14%. On the other hand, the catalyst supported on alumina has greater HYD activity than the catalyst supported on mixed oxide derived from LDH; in this case, the conversions of cyclohexene are 25 and 8.5%, respectively. Thus, the HDS/HYD ratios are 0.6 for sulfide CoMo/ γ -Al₂O₃ and 1.7 for sulfide

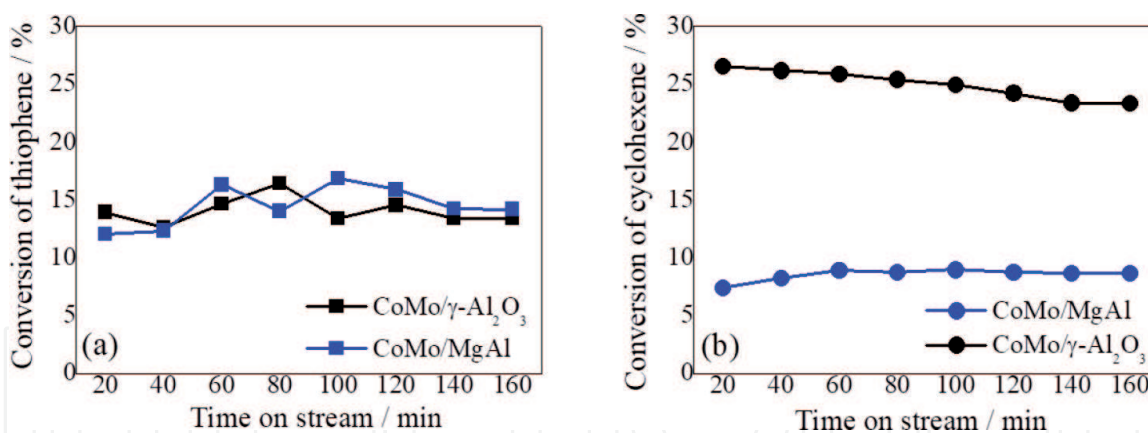


Figure 11.
Conversions of thiophene (a) and cyclohexene (b) for CoMo catalysts.

CoMo/MgAl. This result shows that the catalyst supported on mixed oxide derived from LDH is more selective for HDS reaction.

As in the work of Trejo *et al.* [68], the supported MoO₃ content is approximately 10%. This amount of molybdenum disperses widely in supports containing magnesium, forming MgMoO₄ which are easily sulfided. After sulfidation, the type II CoMoS phase is formed, characterized by promoting high activity for HDS due to the weak interaction with the support, as revealed by Raman spectrum. The opposite effect occurs when the material is supported on alumina, forming connections of the Mo–O–Al type, responsible for making the material sulfidation difficult. The H₂-TPR results corroborate these hypotheses, showing that the catalyst supported on MgAl oxide is reduced at lower temperatures than that supported on alumina, indicating less interaction between this support and the oxide precursor of the active phase.

In summary, supports based on mixed oxides derived from LDHs can be an alternative for use in HDS reactions. Raman spectroscopy is useful in the characterization of the support precursors and, associated with other characterization techniques, it is important in the identification of the active phases.

4. Conclusion

An overview of hydrotalcite-like materials was presented and the most used preparation methods were described. The possibility of varied compositions and their unique structural characteristics make it possible to obtain materials with specific properties and applications in several areas of industrial interest. In catalytic systems particularly these materials are widely studied and several processes need further characterization. In this sense, Raman spectroscopy proves to be an extremely useful and versatile tool, as it can be used for the structural characterization of LDHs, derived mixed oxides, composites, and other materials used. Furthermore, Raman spectroscopy is a very sensitive technique that makes it possible to determine the chemical nature of reaction products, being able to monitor the entire catalytic process. Thereby, the association of Raman with other techniques will allow the evolution in the understanding of different materials and processes.

Acknowledgements

The authors acknowledge the Petrobras for Financial support. Moreover, we would like to express our gratitude toward Prof. Arnaldo C. Faro Jr. (from UFRJ)

for H₂-TPR and HDS catalytic tests facilities, and Prof. Renato B. Guimarães and Jackson A.L.C. Resende (from LDRx/UFF) for providing the XRD facilities.

Conflict of interest

The authors declare no conflict of interest.

IntechOpen

Author details

Luciano Honorato Chagas^{1*}, Sandra Shirley Ximeno Chiaro²,
Alexandre Amaral Leitão¹ and Renata Diniz³

1 Universidade Federal de Juiz de Fora, Juiz de Fora, MG, Brazil

2 Petrobras-CENPES, Rio de Janeiro, RJ, Brazil

3 Universidade Federal de Minas Gerais, Belo Horizonte, MG, Brazil

*Address all correspondence to: hc.luciano@gmail.com

IntechOpen

© 2021 The Author(s). Licensee IntechOpen. This chapter is distributed under the terms of the Creative Commons Attribution License (<http://creativecommons.org/licenses/by/3.0>), which permits unrestricted use, distribution, and reproduction in any medium, provided the original work is properly cited. 

References

- [1] Duan X, Evans D. G, Layered Double Hydroxides: Structure and Bonding. Berlin: Springer-Verlag; 2006. 234 p. DOI: 10.1007/b100426.
- [2] Rives V. Layered Double Hydroxides: Present and Future. New York: Nova Science Publishers, Inc.: 2001. 439 p. ISBN: 978-1-61209-289-8.
- [3] Sun Y, Zhou J, Cheng Y, Yu J, Cai W, Hydrothermal synthesis of modified hydrophobic Zn–Al-layered double hydroxides using structure-directing agents and their enhanced adsorption capacity for nitrophenol. *Adsorpt. Sci. Technol.* 2014;32:351-364. DOI: 10.1260/0263-6174.32.5.351.
- [4] Dos Santos G E S, Dos Lins P V S, De Oliveira L M T M, Da Silva E O, Anastopoulos I, Erto A, Giannakoudakis D A, De Almeida A R F, Da Duarte J L S, Meili L, Layered double hydroxides/ biochar composites as adsorbents for water remediation applications: recent trends and perspectives, *J. Clean. Prod.* 2020;124755. DOI: 10.1016/j.jclepro.2020.124755.
- [5] Soliman H M A, Aly H F, Hydrothermal preparation and characterization of cobased layered double hydroxide and their catalytic activity, *J. Adv. Nanomater.* 2019; 4:1-10. DOI: 10.22606/jan.2019.41001.
- [6] Guo X, Xu S, Zhao L, Lu W, Zhang F, Evans D G, Duan X, One-step Hydrothermal Crystallization of a Layered Double Hydroxide / Alumina Bilayer Film on Aluminum and Its Corrosion Resistance Properties. *Langmuir.* 2009;25:9894-9897. DOI: doi.org/10.1021/la901012w.
- [7] Tao Q, Zhang Y, Zhang X, Yuan P, He H, Synthesis and Characterization of Layered Double Hydroxides With a High Aspect Ratio. 2006;179:708-715. DOI: 10.1016/j.jssc.2005.11.023.
- [8] Ogawa M, Asai S, Hydrothermal synthesis of layered double hydroxide deoxycholate intercalation compounds, *Chem. Mater.* 2000;12:3253-3255. DOI: 10.1021/cm000455n.
- [9] Chagas L H, De Carvalho G S G, Do Carmo W R, San Gil R A S, Chiaro S S X, Leitão A A, Diniz R, De Sena L A, Achete C A, MgCoAl and NiCoAl LDHs synthesized by the hydrothermal urea hydrolysis method: Structural characterization and thermal decomposition. *Mat. Res. Bull.* 2015;64:207-215. DOI: 10.1016/j.materresbull.2014.12.062.
- [10] Mishra G, Dash B, Pandey S, Layered double hydroxides: A brief review from fundamentals to application as evolving biomaterials. *Appl. Clay Sci.* 2018;153:172-186. DOI: 10.1016/j.clay.2017.12.021.
- [11] Barahuie F, Hussein M Z, Gani S A, Fakurazi S, Zainal Z, Synthesis of protocatechuic acid–zinc/aluminium–layered double hydroxide nanocomposite as an anticancer nanodelivery system. *J. Solid State Chem.* 2015;221:21-31. DOI: 10.1016/j.jssc.2014.09.001.
- [12] Olya N, Ghasemi E, Ramezanzadeh B, Mahdavian M, Synthesis, characterization and protective functioning of surface decorated Zn-Al layered double hydroxide with SiO₂ nano-particles. *Surf. Coat. Technol.* 2020;387:125512. DOI: 10.1016/j.surfcoat.2020.125512.
- [13] Crepaldi E L, Pavan P C, Valim J B, Anion exchange in layered double hydroxides by surfactant salt formation. *J. Mater. Chem.* 2000;10:1337-1343. DOI: 10.1039/A909436I.
- [14] Costa D G, Rocha A B, Souza W F, Chiaro S S X, Leitão A A, Ab Initio Study of Reaction Pathways Related to

- Initial Steps of Thermal Decomposition of the Layered Double Hydroxide Compounds. *J. Phys. Chem. C*. 2012;116:13679–13687. DOI: 10.1021/jp303529y.
- [15] Danks A E, Hall S R, Schnepf Z, The evolution of ‘sol–gel’ chemistry as a technique for materials synthesis. *Mater. Horiz.* 2016;3:91-112. DOI: 10.1039/C5MH00260E.
- [16] Mallakpour S, Hatami M, Hussain C M, Recent innovations in functionalized layered double hydroxides: fabrication, characterization, and industrial applications. *Adv. Colloid Interf. Sci.* 2020;283:102216. DOI: 10.1016/j.cis.2020.102216.
- [17] Boehm H P, Steinle J, Vieweger C, $[Zn_2Cr(OH)_6]_x \cdot 2H_2O$, new layer compounds capable of anion exchange and intracrystalline swelling. *Angew. Chemie Int. Ed. English* 1977;16:265-266. DOI: 10.1002/anie.197702651.
- [18] Richetta M, Medaglia P G, Mattoccia A, Varone A, Pizzoferrato R, Layered double hydroxides: tailoring interlamellar nanospace for a vast field of applications. *J. Mater. Sci. Eng.* 2017; 06. DOI: 10.4172/2169-0022.1000360.
- [19] Do Carmo W R, Haddad J F, Chagas L H, Beltrão M S S, De Carvalho G S G, De Oliveira L C A, Souza T E, Leitão A A, Diniz R. Effect of precursor synthesis on the physicochemical properties of Zn–Mg–Al mixed oxides. *Appl. Clay Sci.* 2015;116-117:31-38. DOI: 10.1016/j.clay.2015.08.010.
- [20] Sanati S, Rezvani Z, Ultrasound-assisted synthesis of NiFe-layered double hydroxides as efficient electrode materials in supercapacitors. *Ultrason. Sonochem.* 2018; 48:199-206. DOI: 10.1016/j.ultsonch.2018.05.035.
- [21] Mallakpour S, Dinari M, Behranvand V, Ultrasonic-assisted synthesis and characterization of layered double hydroxides intercalated with bioactive N,N'-(pyromellitoyl)-bis-l- α -amino acids. *RSC Adv.* 2013;3:23303-23308. DOI: 10.1039/c3ra43645d.
- [22] Ay A N, Zümreoglu-Karan B, Mafra L, A simple mechanochemical route to layered double hydroxides: synthesis of hydrotalcite-like Mg-Al-NO₃-LDH by manual grinding in a mortar, *Zeitschrift Für Anorg. Und Allg. Chem.* 2009;635:1470-1475. DOI: 10.1002/zaac.200801287.
- [23] Khusnutdinov V R, Isupov V P, Mechanochemical synthesis of nanocomposites based on Fe₃O₄ and layered double hydroxides. *Mater. Today Proc.* 2019;12:48-51. DOI: 10.1016/j.matpr.2019.03.061.
- [24] Shirin V K A, Sankar R, Johnson A P, Gangadharappa H V, Pramod K, Advanced drug delivery applications of layered double hydroxide. *J. Control. Release* 2021;330:398-426. DOI: 10.1016/j.jconrel.2020.12.041.
- [25] Jin W, Lee D, Jeon Y, Park D-H, Biocompatible Hydrotalcite Nanohybrids for Medical Functions. *Minerals* 2020;10:172. DOI: 10.3390/min10020172.
- [26] Meirelles L M A, Raffin F N, Clay and Polymer-Based Composites Applied to Drug Release: A Scientific and Technological Prospection. *J. Pharm. Pharm. Sci.* 2017; 20:115-134. DOI: 10.18433/J3R617.
- [27] Cao Z, Li B, Sun L, Zhi L L, Xu P, Gu Z, 2D Layered Double Hydroxide Nanoparticles: Recent Progress toward Preclinical/Clinical Nanomedicine. *Small Methods* 2019;1900343. DOI: 10.1002/smt.201900343.
- [28] Dias A C, Fontes M P F, Arsenic (V) removal from water using hydrotalcites as adsorbents: A critical review. *Appl.*

Clay Sci. 2020;191:105615. DOI: 10.1016/j.clay.2020.105615.

[29] Chubar N, Gilmour R, Gerda V, Mičušić M, Omastova M, Heister K, Man P, Fraissard J, Zaitsev V, Layered double hydroxides as the next generation inorganic anion exchangers: Synthetic methods versus applicability. *Adv. Colloid Interface Sci.* 2017;245:62-80. DOI: 10.1016/j.cis.2017.04.013.

[30] Theiss F L, Couperthwaite S J, Ayoko G A, Frost R L, A review of the removal of anions and oxyanions of the halogen elements from aqueous solution by layered double hydroxides. *J. Colloid Interface Sci.* 2014;417:356-368. DOI: 10.1016/j.jcis.2013.11.040.

[31] Mohapi M, Sefadi J S, Mochane M J, Magagula S I, Lebelo K, Effect of LDHs and Other Clays on Polymer Composite in Adsorptive Removal of Contaminants: A Review. *Crystals* 2020;10:0957. DOI: 10.3390/cryst10110957.

[32] Pandey N, Shukla S K, Singh N B, Water purification by polymer nanocomposites: an overview. *Nanocomposites* 2017;3:47. DOI: 10.1080/20550324.2017.1329983.

[33] Wang J, Zhang T, Li M, Yang Y, Lu P, Ning P, Wang Q, Arsenic removal from water/wastewater using layered double hydroxide derived adsorbents, a critical review. *RSC Adv.* 2018;8:22694. DOI: 10.1039/c8ra03647k.

[34] Wang X, Wang H, Wang Y, Gao J, Liu J, Zhang Y, Hydrotalcite/graphene oxide hybrid nanosheets functionalized nanofiltration membrane for desalination. *Desalination* 2019;451:209. DOI: 10.1016/j.desal.2017.05.012.

[35] Tichit D, Layrac G, Gérardin C, Synthesis of layered double hydroxides through continuous flow processes: A review. *Chem. Eng. J.* 2019;369:302. DOI: 10.1016/j.cej.2019.03.057.

[36] Taviot-Guého C, Prévot V, Forano C, Renaudin G, Mousty C, Leroux F, Tailoring Hybrid Layered Double Hydroxides for the Development of Innovative Applications. *Adv. Funct. Mater.* 2017;1703868. DOI: 10.1002/adfm.201703868.

[37] Yan Q, Hou X, Liu G, Li Y, Zhu T, Xin Y, Wang Q, Recent advances in layered double hydroxides (LDHs) derived catalysts for selective catalytic reduction of NO_x with NH₃. *J. Hazard. Mater.* 2020;400:123260. DOI: 10.1016/j.jhazmat.2020.123260.

[38] Lu P, Liu Y, Zhou T, Wang Q, Li Y, Recent advances in layered double hydroxides (LDHs) as two-dimensional membrane materials for gas and liquid separations. *J. Membrane Sci.* 2018;567:89. DOI: 10.1016/j.memsci.2018.09.041.

[39] Hashim N, Sharif S N M, Hussein M G, Isa I M, Kamari A, Mohamed A, Ali N M, Bakar S A, Mamat M, Layered hydroxide anion exchanger and their applications related to pesticides: a brief review. *Mater. Res. Innov.* 2017;21:129. DOI: 10.1080/14328917.2016.1192717.

[40] Wang S, Yang X, Wang F, Song Z, Dong H, Cui L, Effect of modified hydrotalcite on flame retardancy and physical properties of paper. *BioResources* 2019;14:3991. DOI: 10.15376/biores.14.2.3991-4005.

[41] Zhang Z, Qin J, Zhang W, Pan Y-T, Wang D-Y, Yang R, Synthesis of a novel dual layered double hydroxide hybrid nanomaterial and its application in epoxy nanocomposites. *Chem. Eng. J.* 2020;381:122777. DOI: 10.1016/j.cej.2019.122777.

[42] Xie J, Wang H, Wang Z, Zhao Q, Yang Y, Waterhouse G I N, Hao L, Xiao Z, Xu J, Innovative Linear Low Density Polyethylene Nanocomposite Films Reinforced with Organophilic Layered Double Hydroxides:

- Fabrication, Morphology and Enhanced Multifunctional Properties. *Sci. Rep.* 2018;8:52. DOI:10.1038/s41598-017-18811-y. 2002;344:1090-1096. DOI: 10.1002/1615-4169 (200212)344:10<1090::AID-ADSC1090>3.0.CO;2-X.
- [43] Chatterjee A, Bharadiya P, Hansora D, Layered double hydroxide based bionanocomposites. *Appl. Clay Sci.* 2019;177:19. DOI: 10.1016/j.clay.2019.04.022.
- [44] Borges R., Wypych F, Petit E, Forano C, Prevot V, Potential sustainable slow-release fertilizers obtained by mechanochemical activation of MgAl and MgFe layered double hydroxides and K₂HPO₄. *Nanomaterials* 2019;9:183. DOI: 10.3390/nano9020183.
- [45] Bouali A C, Serdechnova M, Blawert C, Tedim J, Ferreira M G S, Zheludkevich M L, Layered double hydroxides (LDHs) as functional materials for the corrosion protection of aluminum alloys: A review. *Appl. Mat. Today* 2020;21:100857. DOI: 10.1016/j.apmt.2020.10085.
- [46] Yan A L, Wang X C, Cheng J P, Research progress of NiMn layered double hydroxides for supercapacitors: A review. *Nanomaterials* 2018;8:747. DOI: 10.3390/nano8100747.
- [47] Lauermannová A-M, Paterová I, Patera J, Skrbek K, Jankovský O, Bartuněk V, Hydrotalcites in Construction Materials. *Appl. Sci.* 2020;10:7989. DOI: 10.3390/app10227989.
- [48] Debecker D P, Gaigneaux E M, Busca G, Exploring, tuning, and exploiting the basicity of hydrotalcites for applications in heterogeneous catalysis. *Chem. Eur. J.* 2009;15:3920-3935. DOI: 10.1002/chem.200900060.
- [49] Climent M J, Corma A, Fornes V, Guil-Lopez R, Iborra S, Aldol condensations on solid catalysts: A cooperative effect between weak acid and base sites. *Adv. Synth. Catal.* 2002;344:1090-1096. DOI: 10.1002/1615-4169 (200212)344:10<1090::AID-ADSC1090>3.0.CO;2-X.
- [50] Choudary B M, Kantam M L, Reddy C R V, Rao K K, Figueras F, The first example of Michael addition catalysed by modified Mg-Al hydrotalcite. *J. Mol. Catal. A Chem.* 1999;146:279-284. DOI: 10.1016/S1381-1169(99)00099-0.
- [51] Pillai U R, Sahle-Demessie E, Sn-exchanged hydrotalcites as catalysts for clean and selective Baeyer-Villiger oxidation of ketones using hydrogen peroxide. *J. Mol. Catal. A Chem.* 2003;191:93-100. DOI: 10.1016/S1381-1169(02)00347-3.
- [52] Climent M J, Corma A, Iborra S, Heterogeneous catalysts for the one-pot synthesis of chemicals and fine chemicals. *Chem. Rev.* 2011;111:1072-1133. DOI: 10.1021/cr1002084.
- [53] Climent M J, Corma A, Iborra S, Mifsud M, Vely A, New one-pot multistep process with multifunctional catalysts: Decreasing the E factor in the synthesis of fine chemicals. *Green Chem.* 2010;12:99-107. DOI: doi.org/10.1039/B919660A.
- [54] Kaneda M, Mizugaki T, Design of high-performance heterogeneous catalysts using hydrotalcite for selective organic transformations. *Green Chem.* 2019;21:1361-1389. DOI: 10.1039/c8gc03391a.
- [55] Homsí D, Rached J A, Aouad S, Gennequin C, Dahdah E, Estephane J, Tidahy H L, Aboukais A, Abi-Aad E, Steam reforming of ethanol for hydrogen production over Cu/Co-Mg-Al-based catalysts prepared by hydrotalcite route. *Environ. Sci. Pollut. Res.* 2017;24:9907-9913. DOI: 10.1007/s11356-016-7480-9.
- [56] Ni M, Leung D Y C, Leung M K H, A review on reforming bio-ethanol for

- hydrogen production. *Int. J. Hydrogen Energy* 2007;32:3238-3247. DOI: 10.1016/j.ijhydene.2007.04.038.
- [57] Haryanto A, Fernando S, Murali N, Adhikari S, Current Status of Hydrogen Production Techniques by Steam Reforming of Ethanol: A Review. *Energy Fuels* 2005;19:2098-2106. DOI: doi.org/10.1021/ef0500538.
- [58] Passos A R, Pulcinelli S H, Santilli C V, Briois V, Operando monitoring of metal sites and coke evolution during non-oxidative and oxidative ethanol steam reforming over Ni and NiCu ex-hydrotalcite catalysts. *Catal. Today* 2019;336:122-130. DOI: 10.1016/j.cattod.2018.12.054.
- [59] Sikander U, Sufian S, Salam M A, A review of hydrotalcite based catalysts for hydrogen production systems. *Int. J. Hydrogen Energy* 2017;42:19851-19868. DOI: 10.1016/j.ijhydene.2017.06.089.
- [60] Zhang G, Zhang X, Meng Y, Pan G, Ni Z, Xia S, Layered double hydroxides-based photocatalysts and visible-light driven photodegradation of organic pollutants: A review. *Chem. Eng. J.* 2020;392:123684. DOI: 10.1016/j.cej.2019.123684.
- [61] Yang Z-Z, Wei J-J, Zeng G-M, Zhang H-Q, Tan X-F, Ma C, Li X-C, Li Z-H, Zhang C, A review on strategies to LDH-based materials to improve adsorption capacity and photoreduction efficiency for CO₂. *Coord. Chem. Rev.* 2019;386:154-182. DOI: 10.1016/j.ccr.2019.01.018.
- [62] Shaw M H, Twilton J, MacMillan D W C, Photoredox Catalysis in Organic Chemistry. *J. Org. Chem.* 2016;81:6898-6926. DOI: 10.1021/acs.joc.6b01449.
- [63] Mohapatra L, Parida K, A review on the recent progress, challenges and perspective of layered double hydroxides as promising photocatalysts. *J. Mater. Chem. A*, 2016;4:10744-10766. DOI: 10.1039/c6ta01668e.
- [64] Jing G, Sun Z, Ye P, Wei S, Liang Y, Clays for heterogeneous photocatalytic decolorization of wastewaters contaminated with synthetic dyes: a review. *Water Practice & Technology* 2017;12:432-443. DOI: 10.2166/wpt.2017.046.
- [65] De Carvalho G S G, Siqueira M M, Nascimento M P, Oliveira M A L, Amarante G W, Nb₂O₅ supported in mixed oxides catalyzed mineralization process of methylene blue. *Heliyon* 2020;6:e04128. DOI: 10.1016/j.heliyon.2020.e04128.
- [66] De Carvalho G S G, Chagas L H, Fonseca C G, De Castro P P, Sant'Ana A C, Leitão A A, Amarante G W, Nb₂O₅ supported on mixed oxides catalyzed oxidative and photochemical conversion of anilines to azoxybenzenes, *New J. Chem.* 2019;43:5863-5871. DOI: 10.1039/c9nj00625g.
- [67] Kaufmann T G, Kaldor A, Stuntz, G F, Kerby M C, Ansell L L, Catalysis science and technology for cleaner transportation fuels. *Catal. Today* 2000;62:77-90. DOI: 10.1016/S0920-5861(00)00410-7.
- [68] Trejo F, Rana M, Ancheyta J, CoMo/MgO-Al₂O₃ supported catalysts: An alternative approach to prepare HDS catalysts. *Catal. Today* 2008;130:327-336. DOI: 10.1016/j.cattod.2007.10.105.
- [69] Brunet S, Mey D, Pérot G, Bouchy C, Diehl F, On the hydrodesulfurization of FCC gasoline: a review. *Appl. Catal. A Gen.* 2005;278:143-172. DOI: 10.1016/j.apcata.2004.10.012.
- [70] Zhao R, Yin C, Zhao H, Liu C, Synthesis, characterization, and application of hydrotalcites in hydrodesulfurization of FCC gasoline. *Fuel Process. Technol.* 2003;81:201-209. DOI: 10.1016/S0378-3820(03)00012-2.

- [71] Coelho T L, Arias S, Rodrigues V O, Chiaro S S X, Oliviero L, Maugé F, Faro Jr A C, Characterisation and performance of hydrotalcite derived CoMo sulphide catalysts for selective HDS in the presence of olefin. *Catal. Sci. Technol.* 2018;8:6204-6216. DOI: 10.1039/c8cy01855c.
- [72] Coelho T L, Micha R, Arias S, Licea Y E, Palacio L A, Faro Jr A C, Influence of the Mg^{2+} or Mn^{2+} contents on the structure of NiMnAl and CoMgAl hydrotalcite materials with high aluminum contents. *Catal. Today* 2015;250:87-94. DOI: 10.1016/j.cattod.2014.07.015.
- [73] Coelho T L, Licea Y E, Palacio L A, Faro Jr A C, Heptamolybdate-intercalated CoMgAl hydrotalcites as precursors for HDS-selective hydrotreating catalysts. *Catal. Today* 2015;250:38-46. DOI: 10.1016/j.cattod.2014.06.016.
- [74] Herrero M, Benito P, Labajos F M, Rives V, Stabilization of Co^{2+} in layered double hydroxides (LDHs) by microwave-assisted ageing. *J. Solid State Chem.* 2007;180:873-884. DOI: 10.1016/j.jssc.2006.12.011.
- [75] Cavani F, Trifirò F, Vaccari A, Hydrotalcite-type anionic clays: Preparation, properties and applications. *Catal. Today* 1991;11:173-301. DOI: 10.1016/0920-5861(91)80068-K.
- [76] Frost R L, Reddy B J, Thermo-Raman spectroscopic study of the natural layered double hydroxide manasseite. *Spectroch. Acta Part A* 2006;65:553-559. DOI: 10.1016/j.saa.2005.12.007.
- [77] Zhang H, Wen X, Wang Y, Synthesis and characterization of sulfate and dodecylbenzenesulfonate intercalated zinc-iron layered double hydroxides by one-step coprecipitation route. *J. Solid State Chem.* 2007;180:1636-1647. DOI: 10.1016/j.jssc.2007.03.016.
- [78] Klopogge J T, Hickey L, Frost R L, The effect of varying synthesis conditions on zinc chromium hydrotalcite: a spectroscopic study. *Mater. Chem. Phys.* 2005;89:99-109. DOI: 10.1016/j.matchemphys.2004.08.035.
- [79] Pradhan J K, Bhattacharya I N, Das S C, Das R P, Panda R K, Characterisation of fine polycrystals of metastable η -alumina obtained through a wet chemical precursor synthesis. *Mater. Sci. Eng.* 2000; B77:185-192. DOI: 10.1016/S0921-5107(00)00486-4.
- [80] Laugier J, Bochu B, Checkcell—A Software Performing Automatic Cell/Space Group Determination, Laboratoire des Matériaux et du Génie Physique de l'Ecole Supérieure de Physique de Grenoble (INPG), France, 2000.
- [81] Constantino V R L, Pinnavaia T J, Basic Properties of $Mg^{2+}_{1-x}Al^{3+}_x$ Layered Double Hydroxides Intercalated by Carbonate, Hydroxide, Chloride, and Sulfate Anions *Inorg. Chem.* 1995;34:883-892. DOI: 10.1021/ic00108a020.
- [82] Crivello M, Pérez C, Fernández J, Eimer G, Herrero E, Casuscelli S, Rodríguez-Castellón E, Synthesis and characterization of Cr/Cu/Mg mixed oxides obtained from hydrotalcite-type compounds and their application in the dehydrogenation of isoamylic alcohol. *Appl. Catal. A Gen.* 2007;317:11-19. DOI: 10.1016/j.apcata.2006.08.035.
- [83] Costa D G, Rocha A B, Diniz R, Souza W F, Chiaro S S X, Leitão A A, Structural Model Proposition and Thermodynamic and Vibrational Analysis of Hydrotalcite-Like Compounds by DFT Calculations. *J. Phys. Chem. C* 2010;114:14133-14140. DOI: 10.1021/jp1033646.
- [84] Farkas L, Gadó P, Werner P E, The structure refinement of Boehmite

- (γ -AlOOH) and the study of its structural variability based on Guinier-Hagg powder data. *Mat. Res. Bull.* 1977;12:1213-1219. DOI: 10.1016/0025-5408(77)90176-3.
- [85] Chagas L H, De Farias S B P, Leitão A A, Diniz R, Chiaro S S X, Speziali N L, De Abreu H A, Mussel W N, Structural comparison between samples of hydrotalcite-like materials obtained from different synthesis route. *Quim. Nova* 2012;35:1112. DOI: 10.1590/S0100-40422012000600008.
- [86] Brühne S, Gottlieb S, Assmus W, Alig E, Schmidt M U, Atomic Structure Analysis of Nanocrystalline Boehmite AlO(OH). *Cryst. Growth Des.* 2008;8:489. DOI: 10.1021/cg0704044.
- [87] Velu S, Suzuki K, Osaki K, Ohashi F, Tomura S, Synthesis of new Sn incorporated layered double hydroxides and their evolution to mixed oxides. *Mater. Res. Bull.* 1999;34:1707-1717. DOI: 10.1016/S0025-5408(99)00168-3.
- [88] Miyata S, Physico-chemical properties of synthetic hydrotalcites in relation to composition. *Clays Clay Miner.* 1980;28:50. DOI: 10.1346/CCMN.1980.0280107.
- [89] Mackenzie K J D, Meinhold R H, Sherriff B L, Xu Z, ^{27}Al and ^{25}Mg Solid-state Magic-angle Spinning Nuclear Magnetic Resonance Study of Hydrotalcite and its Thermal Decomposition Sequence. *J. Mater. Chem.* 1993;3:1263. DOI: 10.1039/JM9930301263.
- [90] Desikan A N, Huang L, Oyama S T, Structure and Dispersion of Molybdenum Oxide Supported on Alumina and Titania, *J. Chem. Soc. Faraday Trans.* 1992;88:3357-3365. DOI: 10.1039/FT9928803357.
- [91] Brown F R, Makovsky L E, Rhee K H, Raman Spectra of Supported Molybdena Catalysts 1. *Oxide Catalysts.* *J. Catal.* 1977;50:162-171. DOI: 10.1016/0021-9517(77)90018-5.
- [92] Radhakrishnan R, Reed C, Oyama S T, Seman M, Kondo J N, Domen K, Ohminami Y, Asakura K, Variability in the Structure of Supported MoO₃ Catalysts : Studies Using Raman and X-ray Absorption Spectroscopy with ab Initio Calculations. *J. Phys. Chem. B* 2001;105:8519-8530. DOI: 10.1021/jp0117361.
- [93] Medema J, Van Stam C, De Beer V H J, Konings A J A, Koningsberger D C, Raman spectroscopic study of CoMo- Al_2O_3 catalysts. *J. Catal.* 1978;53:386-400. DOI: 10.1016/0021-9517(78)90110-0.
- [94] Li X, Chai Y, Liu B, Liu H, Li J, Zhao R, Liu C, Hydrodesulfurization of 4,6-Dimethyldibenzothiophene over CoMo Catalysts Supported on γ -Alumina with Different Morphology. *Ind. Eng. Chem. Res.* 2014;53:9665-9673. DOI: 10.1021/ie5007504.
- [95] Liu X M, Xue H X, Li X, Yan Z F, Synthesis and hydrodesulfurization performance of hierarchical mesopores alumina. *Catal. Today* 2010;158:446-451. DOI: 10.1016/j.cattod.2010.06.032.
- [96] El Kady F Y A, Abd El Wahed M G, Shaban S, Abo El Naga A O, Hydrotreating of heavy gas oil using CoMo/ γ - Al_2O_3 catalyst prepared by equilibrium deposition filtration. *Fuel* 2010;89:3193-3206. DOI: 10.1016/j.fuel.2010.06.024.
- [97] Nava R, Morales J, Alonso G, Ornelas C, Pawelec B, Fierro J L G, Influence of the preparation method on the activity of phosphate-containing CoMo/HMS catalysts in deep hydrodesulphurization. *Appl. Catal. A* 2007;321:58-70. DOI: 10.1016/j.apcata.2007.01.038.